A comparison study of the photocatalytic efficiency of different developed Photocatalysts/polymer composites

Mahmoud Benltifa, Chaima Brahmi, Frédéric Dumur, Lionel Limousy, Latifa Bousselmi, Jacques Lalevée

A comparison study of the photocatalytic efficiency of different developed Photocatalysts/polymer composites

Mahmoud Benltifa[*a], Chaima Brahmi [a,b,c,d], Frédéric Dumur [e], Lionel Limousy [b,c], Latifa Bousselmi [a], Jacques Lalevée*[b,c]*

[a] Laboratory of Wastewaters and Environment, Center for Water Research and Technologies CERTE, BP 273, Soliman 8020, Tunisia

[b] University of Haute-Alsace, CNRS, IS2M UMR 7361, F-68100 Mulhouse, France

[c] University de Strasbourg, France

[d] University of Carthage, National Institute of Applied Sciences and Technology, Tunis 1080, Tunisia

[e] Aix Marseille Univ, CNRS, ICR, UMR7273, F-13397 Marseille, France

[f] Institut Lavoisier Versailles, UMR CNRS 8180, Université de Versailles-St-Quentin-en-Yvelines, Université Paris-Saclay, 78035 Versailles Cedex, France

Correspondence to: M. Benltifa (E-mail: mahmoud.benltifa@certe.rnrt.tn) and J. Lalevée (E-mail: jacques.lalevee@uha.fr)

Keywords: Photocatalysts/polymer composites, Photopolymerization, Photocatalytic degradation.

Abstract

Polyoxometalates (POMs), Metals Organic-Frameworks (MOFs), Perovskites and Oxides are promising crystalline materials that have received increasing attention due to their impressive photocatalytic performances. However, these catalysts are generally produced in powdered form limiting their reuse and recyclability. A recent solution consisted on associating them with an acrylate polymer via a simple, green and rapid photopolymerization process under visible light irradiation. The obtained shaped photocomposites exhibited at the same time the polymer robustness and malleability as well as the photocatalysts remarkable functionalities. The fruitful incorporation of the different crystallites into the polymer matrix, were already reported. However, in order to select the most performant photocatalytic system, which could be probably applied in future

technological environmental applications, it was important to compare the photocatalytic efficiency of the different developed photocomposites. The absorption properties, the reusability and the thermal as well as the mechanical stabilities were taken into account during the in-depth comparison. The MIL-100(Fe)/polymer composite was selected as the most efficient photocatalytic system, which is also reusable during 10 successive catalytic cycles with an observed little decrease in the pollutants final degradation percentages starting from the 8th cycle. Moreover, this Fe-based MOF immobilized photocatalyst is characterized by an interesting mechanical and thermal stabilities as well as a good absorption property allowing its application under visible light irradiation.

1. Introduction

Nowadays, water scarcity, caused by the economic development as well as the continuous use of drugs, plastics, textile dyes and chemicals, represents together a menace for environment, human and living beings[1,2,3,4]. In order to satisfy the increasing demands for clean and safe water, several researchers have focused on the development of new technologies for water depollution. Among these contaminants' elimination methods, the conventional physicochemical approaches such as flocculation, biological treatment, membrane filtration and / or adsorption degrade partially the recalcitrant pollutants[5]. To achieve total mineralization of the targeted compounds, other additional technologies are generally necessary, including advanced oxidation processes, which are based on the production of radicals using photocatalysts, solar energy or lamps[6–9].

The first efficient photocatalytic processes were applying the TiO_2 as photocatalyst. However, this latter, very effective under UV irradiation, absorbs only 4% of the sunlight spectrum, which had led to a continuous development for new catalysts more active under visible light irradiation[10]. The photocatalytic performance depends also on several parameters such as the photocatalysts ability to generate electron-hole pairs with low recombination rates, their absorption and adsorption properties as well as their physical state[11–14]. Therefore various photocatalysts such as polyoxometalates, MOFs, perovskites and oxides were recently applied in composites for the photodegradation of many organic recalcitrant contaminants including pharmaceuticals, textile colorants, herbicides and organic pollutants[15–17]. However, investigations reporting these catalyst composites

application in photocatalysis remain very limited. Markedly, these composites can be generated in mild conditions using photopolymerization processes.

Polyoxometalates are anionic inorganic metal-oxygen clusters in which the coordinated metallic elements in an octahedral environment of oxygen atoms are in a high oxidation state (often d^0 configuration)[18]. These materials are characterized by thermal stability, strong absorption of light in the near UV range as well as a good redox property[19]. These characteristics have allowed their applications in photocatalysis for the degradation of organic pollutants[15], the reduction of heavy metals[20] as well as the reduction of CO_2[21].

The second materials applied as semiconductors belong to the class of coordination polymers also called MOFs (Metal-Organic Frameworks). MOFs are porous crystalline materials formed by a periodic network between metals or metal clusters and organic ligands connected by strong coordination bonds[22]. Depending on the desired applications, several types of MOFs with different properties could be synthesized due to the countless possible combinations between organic ligands and metals[23]. These advantages have enabled these materials application in various fields such as biomedicine for drug delivery, gas storage, separation such as uranium extraction as well as photocatalysis[24].

Perovskites were also very promising candidates due to their chemical and thermal stability, their low synthesis cost as well as their interesting diffusion length allowing a better separation of the generated electrons-holes pairs[25]. A perovskite has generally a cubic crystal structure described by an ABX_3 system, A is a cation larger in size than the cation B and could be either organic such as methyl ammonium (MA^+: $CH_3NH_3^+$) or inorganic such as alkali metals (Na, K) or rare earth metals (La, Sm, Pr). B corresponds to a transition metal ion (Sn, Pb, Ge)[17,26,27]. These catalysts could be applied in many fields, including X-ray imaging[28], photovoltaic cells[17,26] and light-emitting diode (LED) devices[26,29].

More common photo catalysts are metal oxides as TiO_2 and ZnO. In this frame, Manganese oxide, which is, naturally abundant, non-toxic and characterized by an exceptional structural, chemical properties, acid resistance, low cost as well as a narrow band gap energy compared to the TiO_2[30], was chosen as the last photocatalyst to investigate during this study. These nanoparticles are widely applied in various fields including energy storage batteries, imaging, adsorption, sensors and catalysis[31,32]. In fact, the photocatalytic

ability of the manganese oxide was firstly proved two decades ago by Cao and Steven via the oxidation of 2-propanol[33]. Subsequently, this catalyst was applied to degrade various organic compounds including phenol[34], methylene blue[35], rhodamine B[36], indigo carmine dye[31] as well as the diclofenac[37].

The target photocatalysts are green and stable materials. However, they are generally synthesized in powder form, which makes their separation and their regeneration at the end of the photocatalytic process difficult and expensive[38]. An alternative to overcome this problem, to facilitate their technological application and to obtain easily handled and more technologically enhanced systems, was to fix them on solid matrices allowing easier implementation. Several fixation methods are applied to produce films on several substrates and the more used ones are spin coating/deep coating[39–42]. Recent approach has focused on the encapsulation of these photocatalytic powders in different matrix[9,31,43–47]. A polymer synthesized by photopolymerization under LED @ 405 nm irradiation, is used for this purpose and allowed, as well, the control of the final shape in order to improve the photocatalytic activities[9,46,47].. This photopolymerization is more economically advantageous thanks to the possibility of rapid polymers development at room temperature, using low energetic irradiation sources and without causing the emission of volatile organic compounds since the photopolymerizable formulations didn't contain solvents[48,49]. Details about the synthesis, the characterization and the application of the photocatalysts/polymer composites were recently reported in previous investigations[9,46,47,50–52].

Comparison between photocatalysts efficiencies is very difficult as it is strongly depending on several parameters related to photocatalysts chemical and physical properties but also to the operating conditions, the reactor design, the radiation properties, the method of film fixation on the substrate, the film and substrate properties and their interaction. The system is more complex if we consider the properties of the pollutants and their interaction with the photocatalyst system and under the radiation. Depending on the target application of the photocatalytic system, it is important to select the relevant criteria to assess the photocatalytic efficiency of the system. In this study, all the operating conditions, reactor design as well as photocatalyst development are kept constant. The selected criteria for the assessment are photocatalytic efficiencies (first order apparent

constants k_{app})., durability, mechanical properties, band gap energies and the decomposition temperatures of the different developed composites is reported. The final objective is potential real application for water depollution. The specific objective behind the selection of each of these criteria is presented in Table 2. The selected photocatalysts have different structures in order to have wide comparison and are belong to POM, MOF, Perovskites and oxides. Different pollutants are also considered (pharmaceutical, dye as well as plasticizer) and sources of irradiation were taken into consideration during this analysis. Moreover, the results allowed the identification of the advantageous and inconvenient of each photocatalytic system as well as the determination of the most performant and suitable photocomposite for possible future technological applications.

2. Experimental section

2.1. Chemical compounds

The chemicals used for the composite's synthesis are the TMPTA purchased from Allnex, the iodonium hexafluorophosphate (Iod or Speedcure 938) and the phenyl *bis*(2,4,6-trimethylbenzoyl) phosphine oxide (BAPO or Speedcure BPO), obtained from Lambson Ltd (UK) and Allnex.

2.2. Photocomposites synthesis

The different photocomposites were developed via a photopolymerization process, carried out under air by placing the polymerizable resin into a mold (thickness = 1.3 mm). The initial matrix contains the TMPTA as the monomer, the photocatalyst (MOF, POM, Perovskite, Manganese Oxide) as well as the BAPO and the Iodonium salt playing the role of the photoinitiator system. The resin was then irradiated by a Light Emitting Diode emitting at 405 nm (I_0 = 100 mW/cm^2) and the polymerization rates were determined by monitoring of the TMPTA double bond situated at 4730 cm^{-1} for thick samples using a real-time Fourier transform infrared spectroscopy. More details about the development of the photocatalysts/polymer composites were already reported in our previous work[9,46,47].

2.3. Pollutants

The targeted pollutants to degrade in the presence of the photocatalysts/polymer composites are the Acid Black dye, the Bisphenol-A and the Ibuprofen. They were used as benchmark pollutants for these comparisons of photocatalysts/polymer composites.

2.4. Photocatalytic degradation experiments

Photocatalytic efficiency of the photocatalysts/polymer composites were examined via the, Ibuprofen, the Bisphenol-A and the Acid Black photodegradation upon an Omnicure Dynamic lamp, series 1000 lumen (I_0 = 250 mW/cm^2, l = 320-520 nm). The initial concentration and volume of the targeted contaminants solutions were equal to 15 mg/L (24.25 µmol/L) and 4 ml, respectively, since the photocatalytic degradation tests were carried out directly in the analysis cuvette where the photocomposites pellets were added to the aqueous solution. The natural pH of the solutions was equivalent to 5.9, 6.5 and 7.2, respectively for the Acid Black, the Bisphenol-A and the Ibuprofen solutions.

The progress of the model pollutant concentration was investigated by monitoring their absorbances peak over time performed by a JASCO V730 spectrophotometer. The degradation percentages of the contaminants at different illumination times were estimated by the equation below (equation.1):

$$Contaminant\ conversion\ (\%) = (1 - \frac{Abs\ t}{Abs\ t=0}) \times 100 \qquad \text{(equation.1)}$$

Where $Abs\ t = 0$ and $Abs\ t$ are the determined pollutants absorbances before and after a certain time (t) of irradiation.

2.5. Fluorescence experiments

Fluorescence properties of the developed photocomposites were investigated using the JASCO FP-6200 spectrometer (Jasco, Lisses, France).

3. Results and discussion

3.1 Apparent first order of the photodegradation reactions

The photocatalytic efficiency of the different developed composites was the first parameter taken into account during the in-depth comparison carried out between the

various photocatalytic systems, synthesized within our group. The degradation of three Organic pollutants including, the Acid Black dye, the Bisphenol-A and the Ibuprofen were considered and the comparison was based on the first order apparent constants k_{app} calculated for each composite and in the case of each targeted contaminants.

Table 1. Comparison between the photocatalytic efficiencies of the different developed Photocatalysts/polymer composites for the photocatalytic degradation of the Acid Black, the Bisphenol-A and the Ibuprofen. $[Pollutant]_0$ = 15ppm, irradiation source: UV-Visible lamp.

	Acid Black		**Bisphenol-A**		**Ibuprofen**		**Band Gap Energy (e.V)**
	k_{app}(min^{-1}) (60 min)	**R^2**	**k_{app}(min^{-1}) (90 min)**	**R^2**	**k_{app}(min^{-1}) (90 min)**	**R^2**	
$H_3PMo_{12}O_{40}$/polymer	0.051	0.93	0.047	0.97	0.056	0.99	2.8
$Nd_{0.9}TiO_3$/polymer	0.053	0.91	0.061	0.82	0.032	0.93	3.8
$LaTiO_3$/polymer	0.053	0.98	0.038	0.83	0.014	0.94	3.8
MIL-53(Cr)/polymer	0.102	0.94	0.028	0.83	0.015	0.99	2.3
HKUST-1(Cu)/polymer	0.031	0.99	0.016	0.99	0.024	0.99	3.1
MIL-100(Fe)/polymer	0.104	0.98	0.098	0.87	0.106	0.92	2.5
MIL-88A(Fe)/polymer	0.075	0.84	0.023	0.95	0.042	0.94	2.3
MnO_2/polymer	0.049	0.94	-	-	-	-	2.9
TiO_2/polymer	0.007	0.98	0.008	0.98	0.009	0.98	3.2
Polymer	0.007	0.95	0.007	0.99	0.009	0.99	-
Photolysis of the Acid Black only	0.005	0.98	0.005	0.95	0.006	0.94	-

k_{app} = first order apparent kinetic constant.

The Table 1 lists the degradation kinetics of the Acid Black, the Ibuprofen and the Bisphenol-A under UV-Visible lamp irradiation (λ = 320-520 nm, I_0 = 250 mW /cm^2) and in the presence of the different manufactured composites. The photocatalysts mass percentage incorporated in the same acrylic matrix was set at 1%. The comparison was based on the first order apparent constant k_{app}.

Table 1 shows that the various developed composites display interesting photocatalytic activities towards the degradation of the Acid Black dye, the Bisphenol-A and the Ibuprofen. Indeed, these selected compounds were slightly decomposed by simple photolysis under UV-Visible lamp irradiation ($k_{app,\ Acid\ Black}$ = 0.005 min^{-1} vs. 0.104 min^{-1} in the presence of the MIL-100(Fe)/polymer composite for example).

The synthesized composites were more performant than the TiO_2/polymer composite, which was developed under the same experimental conditions than the

Photocatalysts/polymer composites. In fact, in the presence of the MIL-100(Fe)/polymer composite, a first order apparent kinetic constant of 0.104min^{-1} was reached during the decomposition of the Acid Black dye compared to 0.007min^{-1} attained in the presence of the TiO_2/polymer composite. A same kinetic constant value of 0.007min^{-1} was also attained when using the neat polymer matrix, proving that the TiO_2 particles encapsulated into the polymer are not photocatalytically active. This could be explained by their lower shape compared to the other chosen photocatalysts which make them inaccessible once immobilized by the three-dimensional acrylic polymer chains[53].

The obtained results showed that the MIL-100 (Fe) / polymer composite is the best performing one for the decomposition of the three selected organic contaminants. Indeed, this immobilized photocatalyst exhibited an enhanced degradation kinetics compared to that of all other composites (k_{app} Acid Black = 0.104 min^{-1} vs. 0.051 min^{-1} using for example the POM / polymer composite).

3.2 Gap Energy

The better photocatalytic degradation kinetics reached in the presence of the MIL-100(Fe)/polymer composite compared to that achieved in the case of the $H_3PMo_{12}0_{40}$/polymer, Perovskites/polymer MnO_2/polymer and HKUST-1(Cu)/polymer composites, could be explained by its lower gap energy (2.5 eV vs. 2.8, 3.8, 2.9 and 3.1 eV, respectively) (See Table 1). In fact, its absorbance in the UV and up to the visible range covering the entire emission spectrum of the used UV-Visible lamp, makes it more easily excitable by this irradiation source. However, how could we explain the difference between the MIL-88A(Fe)/polymer, the MIL-53(Cr)/polymer and the MIL-100(Fe)/polymer composites, since these three immobilized photocatalysts exhibit approximately similar band gap energies?

In order to elucidate the difference in efficiency between these three composites, fluorescence study has been conducted and the obtained results are represented in Figure 1.

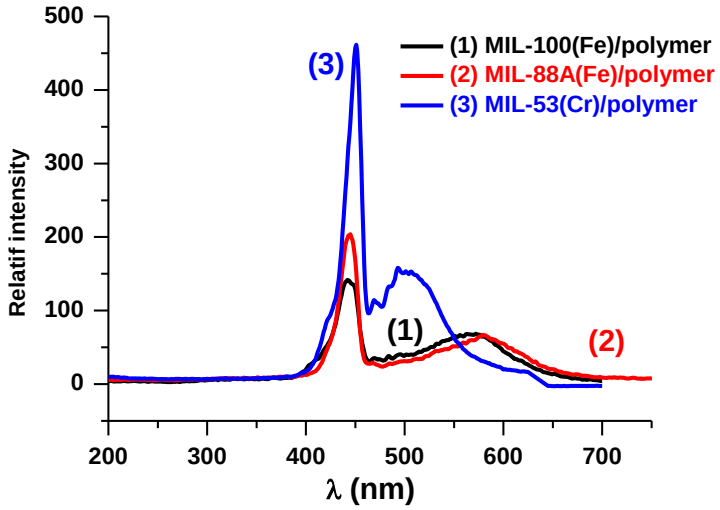

Figure 1. Fluorescence spectra of the composites: (1) MIL-100(Fe)/polymer, (2) MIL-88A(Fe)/polymer et (3) MIL-53(Cr)/polymer. ($\lambda_{excitation}$ = 254 nm).

Figure 1 illustrating the Fluorescence spectra of the different three studied composites, shows that both the MIL-88A(Fe)/polymer and MIL-53(Cr)/polymer composites (blue and red curves) exhibit higher fluorescence intensities than the MIL-100(Fe)/polymer composite (curve in black), reflecting a more rapid recombination of the photogenerated charges formed under irradiation. Therefore, due to its lower band gap energy and fluorescence intensity, the MIL-100(Fe)/polymer composite was the most relevant immobilized photocatalyst for the decomposition of the three targeted organic pollutants.

Details about the degradation mechanisms and the parameters affecting the decomposition behavior of each contaminant were already reported in previous investigations[46,50,52].

3.3 Chemical mechanisms: Involved radicals

Based on the obtained results gathered in Table 2, we can assume that the superoxide anion radicals ($^{\bullet}O_2^-$) are more effective for the pollutants degradation than the hydroxyl and carbonated ones. In fact, these oxygenated radicals are the primal species involved in the pollutants degradation mechanisms in the presence of the most performant composite, the MIL-100(Fe)/polymer.

3.4 Comparison of the catalysts composites: Multi criteria analysis

Moreover, for future technological environmental applications, the chosen photocatalyst should be mechanically and thermally resistant to high water flows and high temperature and should exhibit low band gap energy allowing its activation under visible and solar irradiation. Furthermore, an interesting catalyst should be reusable and photocatalytically active during several catalytic cycles. Consequently, in order to select the most suitable photocomposite for possible forthcoming photocatalytic applications, the mechanical and thermal stabilities, the band gap energies, the durability of the different developed photocomposites and the active species involved in the pollutant's degradation mechanisms were compared. The obtained results are gathered in Table 2.

Table 2. Comparison of the mechanical properties, decomposition temperatures, gap energies, durability and degradation mechanisms of the different studied photocomposites.

	$H_3PMo_{12}O_{40}$/polymer	**$Nd_{0.9}TiO_3$/polymer**	**$LaTiO_3$/polymer**	**MIL-53(Cr)/polymer**	**HKUST-1(Cu)/polymer**	**MIL-100(Fe)/polymer**	**MIL-88A(Fe)/polymer**	**Polymer**
Mechanical properties (G' (MPa))	90	152	154	131	162	139	70	100
Decomposition temperature (°C)	465	478	476	473	467	446	444	475
Band gap energy (eV)	2,8	3,8	3,8	2,3	3,1	2,5	2,3	-
Durability (Number of cycles)	4	8	8	7	8	8	8 (with total deactivation)	-
The radicals involved in the degradation mechanisms	$^{\bullet}OH$	$C^{\bullet}$, $RO^{\bullet}$	$C^{\bullet}$, $RO^{\bullet}$	$C^{\bullet}$, $RO^{\bullet}$, $^{\bullet}OH$	$^{\bullet}OH$, $C^{\bullet}$, $RO^{\bullet}$	$^{-\bullet}O_2$, $C^{\bullet}$, $^{\bullet}OH$, $RO^{\bullet}$	$^{-\bullet}O_2$, $^{\bullet}OH$, $C^{\bullet}$, $RO^{\bullet}$	-

Based on Table 2, it is assumed that the MIL-100(Fe)/polymer composite constitutes the best compromise between the photocatalytic efficiency, the thermal and mechanical stabilities as well as the durability. In fact, in addition to be super active photocatalytically, this photocomposite exhibits interesting storage modulus (G'= 139 MPa), higher than the neat polymer (G'=100 MPa) promoting its application in the photocatalytic field where important flow rates are applied. Moreover, the MIL-100(Fe) immobilized photocatalyst shows high decomposition temperature (446°C) close to the polymer matrix (475°C). Therefore, the thermal resistance of this composite could be attributed to the acrylate

network since the used mass percentage (1%) of the MOFs is too low. Furthermore, due to its low band gap energy (2.5 e.V), this incorporated photocatalyst is expected to be active under natural solar irradiation, which makes it more economically advantageous to use. Furthermore, the manufactured MIL-100(Fe)/polymer composites were used successively during ten successive cycles for the degradation of the Acid Black dye and only a slight decrease of the final decomposition percentages was noticed starting from the 8th cycle.

Table 2 shows also that one of the major drawbacks of the $H_3PMo_{12}O_{40}$/polymer and MIL-88A(Fe)/polymer composites, is essentially their low rigidity characterized by a fairly low storage modulus G' (70 and 90 MPa) compared to the other developed photocomposites. Their durability restricted to 4 cycles in the case of the first immobilized photocatalyst because of the total reduction of molybdenum after irradiation in the presence of the targeted contaminant, was also a considerable usage limit of this POM/polymer composite. This latter, slowly reoxidizes in contact with air but need the addition of oxidative agents such as the hydrogen peroxide for a total reoxidation, which damages and weakens the phosphomolybdic composites surfaces. Moreover, the reuse of the MIL-88A(Fe)/polymer composite was restricted to 8 cycles with total deactivation of the Fe-based MOF, unlike the other composites which still performant even after the 8th photocatalytic cycle. This could be explained by the mechanical fragility (G'=70 MPa) of the immobilized MIL-88A(Fe) photocatalyst. Indeed, this brittleness could provoke the leaching of the MIL-88A (Fe) MOF in the treated solution after several successive cycles of irradiation.

As for the perovskites/polymer composites, their only inconvenient is their absorbance domain limited to the UV region, making them less attractive for environmental photocatalytic application than the other developed systems.

Moreover, the observed diverse degradation mechanisms induced by the studied photocomposites could be explained by the difference in their redox potentials. Further investigations are required in order to better understand the charge exchanges at the composite's interfaces.

Furthermore, the general decline of the photocatalytic performance of the various immobilized photocatalysts, observed starting from the 8th decomposition cycles, could be due to an alteration of the chosen polymer matrix or to the photocatalyst deactivation.

Therefore, improving the polymer resin as well as the regeneration of the catalytic sites are very important prospects to be considered.

4. Conclusions

In conclusion, this study summarized the different results obtained within our group concerning the development of various photocatalysts/polymer composites as well as their application for the degradation of several organic contaminants including the Bisphenol-A, the Ibuprofen and the Acid Black dye.

The in-depth comparison between the different synthesized photocomposites revealed that the MIL-100(Fe)/polymer composite represented the best compromise between efficiency, thermal and mechanical stability, absorption properties as well as reusability. Indeed, this Fe-based MOF composite was characterized by a lower band gap energy (2.5 eV) compared to the POM/polymer, perovskites/polymer and HKUST-1(Cu)/polymer composites. Moreover, the immobilized MIL-100(Fe) exhibited slower recombination of the photogenerated electrons-holes pairs than the MIL-53(Cr)/polymer and MIL-88A(Fe)/polymer composites, which were characterized by band gap energies values equal to 2.3 eV and close to that of the MIL-100(Fe) photocomposite. Moreover, the identified immobilized photocatalyst as the most interesting photocatalytic system exhibited also high decomposition temperature and rigidity allowing it reuse during 10 successive photocatalytic cycles with an observed little decrease in the final degradation percentage starting from the 8^{th} cycle. This decline of the composite photocatalytic ability could be attributed either to the photocatalyst deactivation or to the polymer matrix deterioration. Additional experiments tests should be carried out in order to determine the exact cause of the performances deterioration and to identify the degradation mechanisms involved by each photocatalyst/polymer composite.

The comparison reported in this paper haven't taken into account the development cost of each photocomposites, especially that the most of the used photocatalysts aren't yet commercialized. Therefore, for future environmental technological applications, it will be important to identify the photocatalytic system which represent the best compromise between the photocatalytic efficiency, the reusability and the cost of synthesis.

References

1. Shivaraju, H. P., Midhun, G., Anil Kumar, K. M., Pallavi, S., Pallavi, N., Behzad, S. *Appl Water Sci*, 2017, **7**, 3937–3948.
2. Chander, V., Sharma, B., Negi, V., Aswal, R. S., Singh, P., Singh, R., Dobhal, R. *J Xenobiot*, 2016, **6**.
3. Montes-Grajales, D., Fennix-Agudelo, M., Miranda-Castro, W. *Science of The Total Environment*, 2017, **595**, 601–614.
4. Gupta, N. K., Ghaffari, Y., Kim, S., Bae, J., Kim, K. S., Saifuddin, M. *Scientific Reports*, 2020, **10**, 4942.
5. Sharma, J., Mishra, I. M., Kumar, V. *J. Environ. Manage.*, 2015, **156**, 266–275.
6. Kumar, A., Sharma, G., Naushad, Mu., Al-Muhtaseb, A. H., Kumar, A., Hira, I., Ahamad, T., Ghfar, A. A., Stadler, F. J. *Journal of Environmental Management*, 2019, **231**, 1164–1175.
7. Rani, A., Singh, K., Patel, A. S., Chakraborti, A., Kumar, S., Ghosh, K., Sharma, P. *Chemical Physics Letters*, 2020, **738**, 136874.
8. Zhao, X., Du, P., Cai, Z., Wang, T., Fu, J., Liu, W. *Environmental Pollution*, 2018, **232**, 580–590.
9. Ghali, M., Brahmi, C., Benltifa, M., Dumur, F., Duval, S., Simonnet-Jégat, C., Morlet-Savary, F., Jellali, S., Bousselmi, L., Lalevée, J. *Journal of Polymer Science Part A: Polymer Chemistry*, 2019, **57**, 1538–1549.
10. Dette, C., Pérez-Osorio, M. A., Kley, C. S., Punke, P., Patrick, C. E., Jacobson, P., Giustino, F., Jung, S. J., Kern, K. *Nano Lett.*, 2014, **14**, 6533–6538.
11. Iliev, V., Tomova, D., Todorovska, R., Oliver, D., Petrov, L., Todorovsky, D., Uzunova-Bujnova, M. *Applied Catalysis A: General*, 2006, **313**, 115–121.
12. Iliev, V., Tomova, D., Bilyarska, L., Eliyas, A., Petrov, L. *Applied Catalysis B: Environmental*, 2006, **63**, 266–271.
13. Park, H., Kim, H., Moon, G., Choi, W. *Energy Environ. Sci.*, 2016, **9**, 411–433.
14. Teoh, W. Y., Denny, F., Amal, R., Friedmann, D., Mädler, L., Pratsinis, S. E. *Top Catal*, 2007, **44**, 489–497.
15. Xiuhua, Z., Min, Z., Wei, W. *Chemistry*, 2004, **67**.
16. Chaturvedi, G., Kaur, A., Umar, A., Khan, M. A., Algarni, H., Kansal, S. K. *Journal of Solid State Chemistry*, 2020, **281**, 121029.
17. Das, N., Kandimalla, S. *Int. J. Environ. Sci. Technol.*, 2017, **14**, 1559–1572.
18. Papaconstantinou, E. *Chem. Soc. Rev.*, 1989, **18**, 1–31.
19. Hiskia, A., Mylonas, A., Papaconstantinou, E. *Chem. Soc. Rev.*, 2001, **30**, 62–69.
20. Troupis, A., Gkika, E., Hiskia, A., Papaconstantinou, E. *Comptes Rendus Chimie*, 2006, **9**, 851–857.
21. Guo, S.-X., Li, F., Chen, L., MacFarlane, D. R., Zhang, J. *ACS Appl. Mater. Interfaces*, 2018, **10**, 12690–12697.
22. Xiao, J.-D., Jiang, H.-L. *Acc. Chem. Res.*, 2019, **52**, 356–366.
23. Abdpour, S., Kowsari, E., Moghaddam, M. R. A. *Journal of Solid State Chemistry*, 2018, **262**, 172–180.
24. Genesio, G. phdthesis, Université Montpellier, 2018.
25. Huang, H., Pradhan, B., Hofkens, J., Roeffaers, M. B. J., Steele, J. A. *ACS Energy Lett.*, 2020, **5**, 1107–1123.
26. Dandia, A., Saini, P., Sharma, R., Parewa, V. *Current Research in Green and Sustainable Chemistry*, 2020, **3**, 100031.

27. Eskandari, N., Nabiyouni, G., Masoumi, S., Ghanbari, D. *Composites Part B: Engineering*, 2019, **176**, 107343.
28. Zhou, Y., Chen, J., Bakr, O. M., Mohammed, O. F. *ACS Energy Lett.*, 2021, **6**, 739–768.
29. Adjokatse, S., Fang, H.-H., Loi, M. A. *Materials Today*, 2017, **20**, 413–424.
30. Chiam, S.-L., Pung, S.-Y., Yeoh, F.-Y. *Environ Sci Pollut Res*, 2020, **27**, 5759–5778.
31. Oliveira, L. V. F., Bennici, S., Josien, L., Limousy, L., Bizeto, M. A., Camilo, F. F. *Carbohydrate Polymers*, 2020, **230**, 115621.
32. Dawadi, S., Gupta, A., Khatri, M., Budhathoki, B., Lamichhane, G., Parajuli, N. *Bull Mater Sci*, 2020, **43**, 277.
33. Cao, H., Suib, S. L. *J. Am. Chem. Soc.*, 1994, **116**, 5334–5342.
34. Zhang, Q., Cheng, X., Zheng, C., Feng, X., Qiu, G., Tan, W., Liu, F. *Journal of Environmental Sciences*, 2011, **23**, 1904–1910.
35. Debnath, B., Roy, A. S., Kapri, S., Bhattacharyya, S. *ChemistrySelect*, 2016, **1**, 4265–4273.
36. Cui, H.-J., Huang, H.-Z., Yuan, B., Fu, M.-L. *Geochem Trans*, 2015, **16**, 10.
37. Kuan, W.-H., Liu, Y.-J., Hu, C.-Y. *Int J Environ Res Public Health*, 2020, **17**, 4513.
38. Long, D.-L., Tsunashima, R., Cronin, L. *Angew. Chem. Int. Ed. Engl.*, 2010, **49**, 1736–1758.
39. Tao, C., Wang, J., Chen, R. In *Multilayer Thin Films - Versatile Applications for Materials Engineering*, S. Basu, Ed.; IntechOpen 2020.
40. Sarango, L., Paseta, L., Navarro, M., Zornoza, B., Coronas, J. *Journal of Industrial and Engineering Chemistry*, 2018, **59**, 8–16.
41. Zulkifli, M. H., Bahtiar, A. Jatinangor, Indonesia 2016; 050012.
42. Bayón, R., San Vicente, G., Maffiotte, C., Morales, Á. *Solar Energy Materials and Solar Cells*, 2008, **92**, 1211–1216.
43. Maya, F., Palomino Cabello, C., Figuerola, A., Turnes Palomino, G., Cerdà, V. *Chromatographia*, 2019, **82**, 361–375.
44. Jiang, Y., Mei, C., Zhang, Z., Dong, Z. *Dalton Trans.*, 2021, **50**, 16711–16719.
45. Wu, J., Liao, L., Yan, W., Xue, Y., Sun, Y., Yan, X., Chen, Y., Xie, Y. *ChemSusChem*, 2012, **5**, 1207–1212.
46. Brahmi, C., Benltifa, M., Vaulot, C., Michelin, L., Dumur, F., Millange, F., Frigoli, M., Airoudj, A., Morlet-Savary, F., Bousselmi, L., Lalevée, J. *European Polymer Journal*, 2021, 110560.
47. Brahmi, C., Benltifa, M., Vaulot, C., Michelin, L., Dumur, F., Airoudj, A., Morlet-Savary, F., Raveau, B., Bousselmi, L., Lalevée, J. *European Polymer Journal*, 2021, **157**, 110641.
48. Clapper, J. D., Sievens-Figueroa, L., Guymon, C. A. *Chem. Mater.*, 2008, **20**, 768–781.
49. Purbrick, M. D. *Polymer International*, 1996, **40**, 315–315.
50. Brahmi, C., Benltifa, M., Ghali, M., Dumur, F., Simonnet-Jégat, C., Monnier, V., Morlet-Savary, F., Bousselmi, L., Lalevée, J. *J Appl Polym Sci*, 2021, 50864.
51. Ghali, M., Brahmi, C., Benltifa, M., Vaulot, C., Airoudj, A., Fioux, P., Dumur, F., Simonnet-Jégat, C., Morlet-Savary, F., Jellali, S., Bousselmi, L., Lalevée, J. *Journal of Polymer Science*, 2020, pol.20200568.
52. Brahmi, C., Benltifa, M., Ghali, M., Dumur, F., Simonnet-Jégat, C., Valérie, M., Morlet-Savary, F., Bousselmi, L., Lalevée, J. *Journal of Environmental Chemical Engineering*, 2021, **9**, 106015.
53. Sungur, Ş. In *Handbook of Nanomaterials and Nanocomposites for Energy and Environmental Applications*, O. V. Kharissova, , L. M. T. Martínez, and B. I. Kharisov, Eds.; Springer International Publishing, Cham 2020; pp. 1–18.